

# Spatial correlations in hexagons generated via a Kerr nonlinearity

Alessandra Gatti<sup>1</sup> and Stefano Mancin<sup>2</sup>

<sup>1</sup> INFN, Dipartimento di Scienze, Università dell'Insubria, Via Valleggio 11, I-22100 Como, Italy

<sup>2</sup> INFN, Dipartimento di Fisica, Università di Milano, Via Celoria 16, I-20133 Milano, Italy  
(April 17, 2024)

We consider the hexagonal pattern forming in the cross-section of an optical beam produced by a Kerr cavity, and we study the quantum correlations characterizing this structure. By using arguments related to the symmetry broken by the pattern formation, we identify a complete scenario of six-mode entanglement. Five independent phase quadratures combinations, connecting the hexagonal modes, are shown to exhibit sub-shot-noise fluctuations. By means of a non-linear quantum calculation technique, quantum correlations among the mode photon numbers are demonstrated and calculated.

42.50.Lc, 42.50.Ne, 42.65.Jx

## I. INTRODUCTION

It is well-known that spatial patterns may arise spontaneously in the transverse cross-section of optical beams as a consequence of nonlinear wave mixing processes [1]. Equally fascinating, by maybe less known, is the presence of highly non-classical spatial correlations in the beam cross-section, underlying the classical process of pattern formation. In optical systems the nonlinearity is associated with the simultaneous absorption and emission of a number of photons, a circumstance that creates entanglement among the waves that form the pattern. On a macroscopic level, this is at the very origin of non-classical spatial correlations in the transverse far-field plane [1b].

Among the possible spatial structures that may spontaneously arise in a beam cross section, the hexagonal pattern is one of the most common ones. Hexagonal structures have been predicted to form, typically, in Kerr or Kerr-like media in various configurations. These include counterpropagating waves interacting with a slice of Kerr material in a cavityless configuration [2], systems with a single feedback mirror [3], and planar resonators filled with a self-focusing Kerr medium [4], or with a non-saturable absorber [5]. Experimental observations of this kind of optical pattern include counterpropagating beams in sodium [6], and a variety of systems with single feedback (see e.g. [7]).

This paper is devoted to the analysis of the quantum properties of the hexagonal pattern, in the context of a model for a Kerr medium enclosed in a planar resonator driven by a plane-wave pump beam. This model represents, for its simplicity, a paradigm for optical pattern formation. In fact, it was one of the first models able to predict a transverse modulational instability in an optical system [9]. If only one dimension in the transverse plane is considered [9], the modulational instability gives origin to a roll pattern in the near field immediately out of the cavity. The two dimensional version of the model, analysed by [4], predicts that, above a suitable threshold of the input intensity, a spontaneous breaking of the translational symmetry in the transverse plane gives rise to a hexagonal pattern in the near field, which in the far field corresponds to six bright spots in hexagonal arrangement surrounding a central spot.

Quantum aspects of the hexagonal pattern in the Kerr cavity were first evidenced by Grynberg and Lugiato [10]. Quantum correlations in the light intensities of groups of four among the six hexagonal spots were predicted by using momentum-energy conservation arguments, which did not take into account the effects of dissipation through the cavity mirror (hence valid only for a single pass through the nonlinear medium).

As in the approach of [10] we will restrict our analysis to a seven-mode model, valid close to the instability threshold. By using a quantum calculation technique which takes into account the full nonlinearity of the problem, we will be able to demonstrate that the results of [10], hold also in the presence of cavity dissipation. Moreover, we will derive an analytical formula for the fluctuation spectrum describing the quantum correlation among mode intensities.

In the second part of the paper we will resort to more traditional calculation technique, namely to the usual linearization of the quantum fluctuation dynamics around the classical steady-state pattern. By using arguments related to the translational symmetry of the model, broken by the pattern formation, we shall identify a complete scenario of quantum correlation among the phase quadratures of the six hexagonal modes.

We believe that the six mode entanglement described in this paper, besides being likely to be accessible to experiments, might be of relevance from the point of view of quantum information applications.

Section II introduces the quantum mechanical and classical models describing the self focusing Kerr cavity. Section III is devoted to photon number correlations among the hexagonal modes in the context of a nonlinear model. Section IV investigates in general the phase quadrature correlation among modes. Section V concludes and discusses open questions.

## II. THE MODEL

In this section we present the quantum mechanical counterpart [11] of a well-known semi-classical model [9,4], which describes the dynamics of the scalar electric field in a cavity filled with an isotropic Kerr medium.

We consider a one-directional planar cavity (Fig. 1), with a single input-output port, driven by a coherent, plane-wave, monochromatic field of frequency  $\omega_0$ . The model is derived in the framework of the slowly varying envelope and paraxial approximation, and of the cavity mean field limit [12], which allows to neglect the dependence of the field on the longitudinal coordinate  $z$  along the sample. Under these assumptions only one longitudinal cavity mode is relevant, precisely the one corresponding to the longitudinal cavity resonance  $\omega_c$  closest to  $\omega_0$ . We denote by  $A(\mathbf{x};t)$  the intracavity field envelope operator corresponding to this mode; it depends on the transverse space coordinate  $\mathbf{x} = (x; y)$  and time  $t$ , and obey standard equal-time commutation relations

$$A(\mathbf{x};t); A^\dagger(\mathbf{x}^0;t) = (\mathbf{x} - \mathbf{x}^0): \quad (1)$$

By adopting a picture where the fast oscillation at the carrier frequency  $\omega_0$  is eliminated, the reversible part of the intracavity field dynamics is governed by the three Hamiltonian terms

$$H = H_{\text{free}} + H_{\text{ext}} + H_{\text{int}}: \quad (2)$$

The coupling due to the Kerr nonlinearity in the medium is accounted for by

$$H_{\text{int}} = \hbar \frac{g}{2} \int d^2\mathbf{x} A^\dagger(\mathbf{x})^2 A(\mathbf{x})^2 \quad (3)$$

where the coupling constant  $g$  is proportional to the third order  $^{(3)}$  susceptibility, and  $\int d^2\mathbf{x}$  is the cavity linewidth. This Hamiltonian describes four-wave-mixing interactions at a microscopic level, where they correspond to simultaneous annihilation and creation of photons in pairs [11]. Free propagation in a planar cavity is described, in the paraxial approximation, by

$$H_{\text{free}} = \hbar \int d^2\mathbf{x} A^\dagger(\mathbf{x}) \left( -\frac{1}{2} \nabla_{\perp}^2 \right) A(\mathbf{x}); \quad (4)$$

where  $\Delta$  is the cavity detuning parameter; the two dimensional transverse Laplacian  $\nabla_{\perp}^2 = \frac{\partial^2}{\partial x^2} + \frac{\partial^2}{\partial y^2}$  models the effect of diffraction in the paraxial approximation; the parameter  $l_D = \frac{L}{2T}$ , with  $L$  being the light wavelength,  $L$  the total cavity length, and  $T$  the transmittivity coefficient of the cavity input-output mirror, defines the characteristic length scale for transverse pattern formation. Finally, the coherent pumping, by a classical plane-wave driving field of amplitude  $E_{\text{in}}$ , is modeled by the term:

$$H_{\text{ext}} = i\hbar \int d^2\mathbf{x} [E_{\text{in}} A^\dagger(\mathbf{x}) - E_{\text{in}}^* A(\mathbf{x})]: \quad (5)$$

Dissipation through the cavity mirror can be described in the framework of standard cavity input-output formalism (see e.g. [13]). As a result the dynamics of the intracavity envelope operator is governed by the equation

$$\frac{\partial}{\partial t} A(\mathbf{x};t) = \left( -\frac{1}{2} \nabla_{\perp}^2 - \Delta \right) A(\mathbf{x};t) - ig A(\mathbf{x};t)^\dagger A(\mathbf{x};t) A(\mathbf{x};t) - \sqrt{\frac{\gamma}{2}} A_{\text{in}}(\mathbf{x};t); \quad (6)$$

where the noise operator  $A_{\text{in}}(\mathbf{x};t)_{\text{in}}$  represents the vacuum fluctuations entering the cavity input-output mirror. It has zero mean, and obeys the free field commutation relation

$$[A_{\text{in}}(\mathbf{x};t); A_{\text{in}}^\dagger(\mathbf{x}^0;t^0)] = (\mathbf{x} - \mathbf{x}^0) \delta(t - t^0): \quad (7)$$

Equation (6) must be coupled with the relation at the cavity mirror, linking the outgoing reflected field  $A_{\text{out}}(\mathbf{x};t)$  with the intracavity and input fields

$$A_{\text{out}}(\mathbf{x};t) = \sqrt{\frac{\gamma}{2}} A(\mathbf{x};t) - A_{\text{in}}(\mathbf{x};t); \quad (8)$$

where, in our notation, the total input field operator is given by  $A_{\text{in}}(\mathbf{x};t) = \sqrt{2}E_{\text{in}} + A_{\text{in}}(\mathbf{x};t)$ .

The classical counterpart of this model is the well known partial differential equation [9]

$$\frac{1}{\partial t} \frac{\partial E}{\partial t} = -E + E_{in} + i \mathcal{E} \mathcal{E}^{\dagger} + \frac{1}{2} r^2 E - E; \quad (9)$$

for the envelope of the classical electric field  $E$ . This equation is straightforwardly obtained by its operatorial version (6) by dropping the noise term, and scaling the input and intracavity field intensities to the saturation photon number  $1=g$ , i.e.  $g\mathcal{E}\mathcal{E}^{\dagger} \rightarrow \mathcal{E}\mathcal{E}^{\dagger}$ ,  $g\mathcal{E}_{in}\mathcal{E}^{\dagger} \rightarrow \mathcal{E}_{in}\mathcal{E}^{\dagger}$ .

Since the model has an overall translational symmetry in the transverse plane, equation (9) admits a transversely homogeneous stationary solution  $E_{0s}$ , which obeys the well-known cubic steady-state equation [14]

$$\mathcal{E}_{in}\mathcal{E}^{\dagger} = \mathcal{E}_{0s}\mathcal{E}^{\dagger} + \frac{1}{2} \mathcal{E}_{0s}\mathcal{E}^2: \quad (10)$$

As shown by Lugiato and Lefever [9], by increasing the input intensity a spontaneous breaking of the translational symmetry occurs, and the steady state (10) becomes unstable with respect to perturbations spatially modulated in the transverse plane. As it is common in pattern formation processes [1] the instability develops with a definite critical wave number  $k_c$ , which characterizes the periodicity of the pattern immediately above the instability threshold. The critical point for the onset of the modulational instability is given by [9]

$$\mathcal{E}_{0s}\mathcal{E}^{\dagger} = 1; \quad \frac{1}{2} k_c^2 = 2 \quad : \quad (11)$$

Among the transverse modes on the critical circle  $k_j = k_c$ , the Kerr nonlinearity selects a discrete set of six wave vectors [4,15], so that immediately above the critical point the near field intensity distribution consists of a hexagonal lattice of bright spots, while the far field shows a central bright spot surrounded by six spots in hexagonal arrangement.

The origin of this particular pattern can be understood by considering the microscopic processes leading to on-axis emission of photons allowed by energy-momentum conservation [16]. By referring to the scheme of figure 2a, a first process that preserves the radiation transverse momentum involves destruction of two photons of the plane-wave input beam, and creation of two photons propagating on-axis in symmetric directions. This is the only possible process in a 1-D version of this model [9], and would lead to the formation of a stripe pattern in the near field, as e.g. predicted by a vectorial model for a self-defocusing Kerr medium [17,18], or in the case of a degenerate optical parametric oscillator [19]. In this system, however, the stripe pattern is unstable, because secondary four-wave mixing processes can take place. By referring to figure 2, we can e.g. consider destruction of one on-axis photon of the input beam and one photon propagating in direction 1, and creation of two on-axis photons propagating in directions 2 and 6. By considering also the symmetric process, that involves destruction of a photon in mode 4 and one in the on-axis mode, and creation of two photons in mode 3 and 6, respectively, we see that the six on-axis hexagonal modes are activated. Close to the threshold for pattern formation, all the other processes allowed by energy-momentum conservation, that do not involve on-axis photons, can be neglected, because on-axis mode intensities are much weaker than that of the on-axis homogeneous mode, where the pump beam is injected.

### III. PHOTON NUMBER CORRELATION IN THE HEXAGONAL PATTERN

The microscopic processes which generate the hexagonal pattern are at the origin of non-classical correlation among different portions of the far-field cross section. Referring to the example of figure 2, it can be noticed that whenever two photons are detected at positions 2 and 3 in the far field, there must be two other photons at position 5 and 6, which suggests the existence of a high level of correlation between the sum of photon numbers  $N_2 + N_3$  and  $N_5 + N_6$  (the same reasoning can be applied to any symmetric group of four spots).

A more quantitative argument for the existence of such a kind of intensity correlation in the hexagonal pattern was given by Grynberg and Lugiato [10]. They considered a discrete model for the hexagonal pattern formation in Kerr media, which takes into account only the six hexagonal modes plus the homogeneous mode  $k=0$ , valid close to the threshold for pattern formation, where these modes give the most relevant contribution to the system dynamics. By considering a quantization box in the transverse plane of side  $b$  ( $b \rightarrow 1$  at the end of the calculations) they set

$$A(\mathbf{x};t) = \frac{1}{b} a_0(t) + \frac{1}{b} \sum_{i=1}^6 a_i(t) e^{i\mathbf{k}_i \cdot \mathbf{x}}; \quad (12)$$

with (see figure 2b)  $\mathbf{k}_1 = (0; k_c)$ ,  $\mathbf{k}_2 = (k_c/2; \sqrt{3}/2 k_c)$ ,  $\mathbf{k}_3 = (k_c/2; -\sqrt{3}/2 k_c)$ ,  $\mathbf{k}_4 = -\mathbf{k}_1$ ,  $\mathbf{k}_5 = -\mathbf{k}_2$ ,  $\mathbf{k}_6 = -\mathbf{k}_3$ . By inserting this expansion into the system Hamiltonian (2) they found that the combination of mode photon numbers

$$N_i = N_{i+1} + N_{i-1} - (N_{i+3} + N_{i-4}); \quad i = 1; \dots; 6; \quad i \rightarrow j \equiv i + j \text{ mod } 6 \quad (13)$$

with  $N_i = a_i^\dagger a_i$ , commutes with the discretized Hamiltonian. Thus, in a single pass through the nonlinear medium the observable  $N_i$  is preserved. If there are no photons in the hexagonal modes at the crystal entrance, perfect correlation is found at the exit between e.g.  $N_i + N_{i+1}$  and  $N_{i+3} + N_{i+4}$ . However, when the crystal is inserted in an open resonator, the field is recycled by the cavity and dissipation through the cavity input/output mirror should be taken into account. As a matter of fact, the release of a photon out of the cavity mirror is a random process uncorrelated with the nonlinear processes taking place in the crystal, so that one would expect that cavity dissipation is detrimental for this kind of correlation.

However, we will now show that this is not the case. In order to elucidate this point, we shall follow two different techniques. The standard one, which will be employed in the next section, makes use of the small quantum noise approximation, and consists of linearizing the dynamics of quantum fluctuations around a classical steady state. The other one consists of trying to solve the non-linear Langevin equations that govern the dynamics of the photon number operators of the hexagonal modes. These equations take the general form (see e.g. [13])

$$\frac{d}{dt}N_i = -2N_i + \frac{1}{i\hbar}[N_i; H] + \frac{\hbar}{2}a_i^\dagger a_i^{\text{in}} + a_i^{\text{in}} a_i \quad (14)$$

with  $a_i^{\text{in}}$  being noise operators modelling the vacuum input fluctuations on  $i$ -th mode. They obey standard free-field commutation rules

$$[a_i^{\text{in}}(t); a_j^{\text{in}}(t^0)] = i\delta_{ij} \delta(t - t^0) \quad (15)$$

and have the noticeable commutator with a generic intracavity operator  $O$  [13]

$$[O(t); a_i^{\text{in}}(t^0)] = \frac{\hbar}{2} \theta(t - t^0) [O(t); a_i(t^0)] ; \quad (16)$$

where  $\theta$  is the step function. Equation (16) expresses the fact that intracavity operators at time  $t$  commute with the input operator at a later time  $t^0$  due to causality. The discretized version of Hamiltonian (3), obtained by means of the expansion (12), results [10]

$$H_{\text{int}} = H_{\text{SPM}} + H_{\text{CPM}} + H_{\text{FWM}}^{(1)} + H_{\text{FWM}}^{(2)} + H_{\text{FWM}}^{(3)} ; \quad (17)$$

where  $H_{\text{SPM}}$  describes self-phase modulation

$$H_{\text{SPM}} = \hbar \sum_{j=0}^X \frac{g^6}{2} a_j^{\dagger 2} (a_j)^2 ; \quad (18)$$

while  $H_{\text{CPM}}$  describes cross-phase modulation

$$H_{\text{CPM}} = 2\hbar g \sum_{i < j}^X a_i^\dagger a_i a_j^\dagger a_j ; \quad (19)$$

and  $H_{\text{FWM}}$  describes four-wave mixing

$$H_{\text{FWM}}^{(1)} = \hbar g^4 \sum_{j=1}^X a_0^2 a_j^\dagger a_j^\dagger a_j a_j + \text{h.c.} ; \quad (20)$$

$$H_{\text{FWM}}^{(2)} = 2\hbar g^4 \sum_{i < j}^X a_i a_{i+3} a_j^\dagger a_j^\dagger a_j a_j + \text{h.c.} ; \quad (21)$$

$$H_{\text{FWM}}^{(3)} = 2\hbar g^4 \sum_{j=1}^X a_0 a_j a_{j+1}^\dagger a_{j+5}^\dagger + \text{h.c.} ; \quad (22)$$

Other terms of the Hamiltonian commute with the photon number operators.

The second term at RHS of the dynamical equations (14) is therefore a complicated expression, involving third order products of mode operators, so that finding an explicit solution seems unlikely. However, when considering the combination of mode photon numbers  $N$  given by Eq.(13) the dynamics drastically simplify:

$$\frac{d}{dt}N = 2N - \frac{i}{\hbar} [N, H] + \frac{P}{2} \overline{G} ; \quad (23)$$

$$= 2N + \frac{P}{2} \overline{G} ; \quad (24)$$

where we used the fact that  $N$  commutes with the system Hamiltonian, and the operator  $G$  is defined as:

$$G = a_i^y a_i^{in} + a_i^{y in} a_i + a_{i-1}^y a_{i-1}^{in} + a_{i-1}^{y in} a_{i-1} \\ + a_{i+3}^y a_{i+3}^{in} + a_{i+3}^{y in} a_{i+3} + a_{i+4}^y a_{i+4}^{in} + a_{i+4}^{y in} a_{i+4} \quad (25)$$

When the input operators of the hexagonal modes are in the vacuum state,  $\langle G(t) \rangle = 0$ . Moreover, by using

i) the commutation relations of input operators,

ii) the causality relations expressed by Eq. (16),

iii) the fact that the  $a_i^{in}$  annihilates the vacuum on the right and  $a_i^{y in}$  the vacuum on the left,

it is not difficult to show that

$$\langle G(t) G(t') \rangle = \langle G(t) \rangle \langle G(t') \rangle = 0 ; \quad (26)$$

with

$$N_+ = N_i + N_{i-1} + N_{i+3} + N_{i+4} ; \quad (27)$$

At steady state  $\langle N_+(t) \rangle$  does not depend on time and Eq.(24) is easily solved in the frequency domain. By setting

$$N_+(\omega) = \int_{-\infty}^{\infty} dt \frac{d}{dt} N_+(t) e^{i\omega t} ; \quad (28)$$

we have

$$N_+(\omega) = \frac{P}{2} \frac{\overline{G}(\omega)}{i\omega} ; \quad (29)$$

By using the boundary relations for the outgoing mode operators  $a_i^{out} = a_i - \frac{P}{2} \overline{a_i^{in}}$ , we get

$$N^{out}(\omega) = 2N_+(\omega) + N^{in}(\omega) - \frac{P}{2} \overline{G}(\omega) = \frac{P}{2} \overline{G}(\omega) \frac{i\omega}{2 - i\omega} + N^{in}(\omega) ; \quad (30)$$

The fluctuation spectrum of the output photon number combination  $N^{out}$  can now be calculated as:

$$V(\omega) = \int_{-\infty}^{\infty} dt \langle N^{out}(t) N^{out}(0) \rangle e^{i\omega t} = \hbar N_+ i \frac{4}{\omega^2 + 4} ; \quad (31)$$

where  $N^{out} = N^{out} - \langle N^{out} \rangle$ . Hence the noise spectrum of  $N^{out}$  turns out to have a standard Lorentzian shape [11], with the Lorentzian dip well below the shot-noise level represented by  $2\hbar N_+ i = \hbar N_+^{out} i$ . This result is reminiscent of the "two in beam" correlation spectrum calculated for the down-converted fields generated by a parametric oscillator without spatial aspects [20]. As a matter of fact, in the case of two in beam generation, the photon number difference between the two beams has zero commutator with the system Hamiltonian. The calculation of the noise spectrum of the number difference may be performed following exactly the same steps outlined here, and it is not a coincidence that the result turns out to be the same. However, in contrast to the more standard method of analysis, which exploits the small quantum noise limit by linearizing the model equations around a classical steady-state, the method used

here is "exact", because it takes into account the full nonlinearity, and does not depend on the particular steady state chosen.

In this connection it should be noted that our result concerning spatial intensity correlation in the hexagonal pattern is valid both above and below the threshold for pattern formation, where there is no classical pattern at all.  $O$ -axis emission of photons is here generated purely by quantum fluctuations; on average translational and rotational symmetry are preserved, so that  $o$ -axis photons can be emitted in any direction. However, the mechanism of photon absorption and emission is such to preserve the transverse radiation momentum; as a consequence any six regions in hexagonal arrangement with arbitrary orientation in the far field plane display exactly the same kind of intensity correlation that we have described above threshold.

Incidentally, it is worth noting that the same method can be applied to analyze the quantum spatial correlation in the far field plane of the down-converted field emitted by an optical parametric oscillator, where under proper circumstances the downconverted field is emitted in the form of two plane waves slightly tilted with respect to the cavity longitudinal axis [19]. By interference these two waves give rise in the near field to a stripe pattern, while the far-field intensity distribution consists of two symmetrical spots. From a microscopic point of view, the most relevant three-wave-mixing process close to threshold involves destruction of a pump photon that propagates longitudinally, and creation of two down-converted photons propagating in symmetrical directions, as it is required by transverse momentum conservation. Hence, the two  $o$ -axis signal waves emitted above threshold are made of twin photons and the photon numbers  $N_1; N_2$  that cross in the unit time two ideal detectors surrounding the two spots in the far field plane are highly correlated [21, 24]. In the framework of a three-mode model, valid close to threshold, a calculation analogous to that performed in the case of hexagons shows that the noise spectrum of their difference  $N = N_2 - N_1$  is given exactly by the formula (31).

A last interesting remark is the following: in the Kerr cavity model, when the quantum fluctuation dynamics is linearized around the homogeneous steady-state below threshold, intensity correlation is found between any two symmetric wave-vectors  $\mathbf{k}$  and  $-\mathbf{k}$  close to the critical circle, just as in the case of parametric down-conversion. Hence the linear analysis does not give any hint about the existence of a hexagonal pattern above threshold, with its quantum correlations. This is not in contradiction with our result, since quantum correlation between two symmetric modes obviously implies a noise reduction in the observable  $N$  connecting two couples of symmetric modes. However, the inverse is not in general true. Since the intensity difference between symmetric modes is not a constant of motion of the full Hamiltonian, we expect that the level of correlation between symmetric modes decreases when approaching the region where linearization fails, that is, in the neighbourhood of the instability point, where the size of fluctuations increases, or for a truly microscopic system characterized by a small saturation photon number parameter. On the contrary, our non-linear analysis shows that the correlations which are at the origin of noise suppression in  $N$  do not depend on the distance from threshold or on the system size.

#### IV. PHASE QUADRATURE CORRELATION IN THE HEXAGONAL PATTERN

In the previous section it has been demonstrated a high level of intensity correlation in groups of four among the hexagonal modes. A natural question which arises is whether there exist any other kind of correlation among the six modes at the quantum level. This possibility is suggested by the example of twin beams generation. In fact, in this case, not only the photon number fluctuations are correlated, but also the "phase" fluctuations of the two beams are anti-correlated at a quantum level. To be more precise, there exist two orthogonal field quadratures of the two beams which show, at the same time, a high level of (anti)correlation. This is at the origin of the EPR aspects of the twin beams [25, 26], which are widely exploited in the field of quantum information with continuous variables (see e.g. [27, 29]).

Since we do not have in mind other constant of motion (other observable commuting with the Hamiltonian), we have to resort to traditional means of calculations. Namely, in the framework of the seven-mode discrete model (12), we separate the quantum fluctuation operator from the classical mean field

$$a_i(t) = \frac{1}{\sqrt{g}} \tilde{a}_i(t) + \bar{a}_i(t) \quad i = 0; 1; \dots; 6 \quad (32)$$

---

<sup>1</sup>More precisely, it is exact as long as transverse modes other than those forming the pattern at the instability onset are negligible.

where  $a_j$  are the classical steady state amplitudes of the seven modes. More precisely, they are the steady state solution of a set of classical dynamical equation, obtained by introducing in Eq.(9) the discrete expansion of the envelope operator  $E(\mathbf{x};t) = \frac{1}{b} a_0(t) + \frac{1}{b} \sum_{i=1}^6 a_i(t) e^{i\mathbf{k}_i \cdot \mathbf{x}}$ . These equations have the form :

$$\begin{aligned} \frac{1}{b} \frac{d}{dt} a_0 &= E_I - (1 + i) a_0 + i a_0^2 + 2i \sum_{j=1}^6 a_j a_j^* + i \sum_{j=1}^6 a_0 a_j a_j^* + 2i \sum_{j=1}^6 a_j a_j a_j^* ; \\ \frac{1}{b} \frac{d}{dt} a_j &= (1 + 2i) a_j + i a_j^2 + 2i \sum_{i \neq j}^6 a_i a_j^* + 2i a_j \sum_{i \neq j}^6 a_i a_i^* + 2i a_j a_0 a_0^* + 2i a_j a_0 a_0^* + 2i a_j a_0 a_0^* ; \quad j = 1, \dots, 6 ; \end{aligned} \quad (33)$$

where we took into account the fact that all the hexagonal modes have the same critical transverse wave number, such that  $k_D^2 + 1_D^2 k_C^2 = 2$ .

By inserting the expansion (12) into the model equation (6), with the ansatz (32), and keeping only the leading terms in the small quantum fluctuations we are left with a problem of the form

$$\begin{pmatrix} \frac{d}{dt} \\ \vdots \\ \frac{d}{dt} \end{pmatrix} \begin{pmatrix} a_0 \\ \vdots \\ a_6 \end{pmatrix} = \begin{pmatrix} 14 & 14 \\ \vdots & \vdots \end{pmatrix} \begin{pmatrix} a_0 \\ \vdots \\ a_6 \end{pmatrix} + \frac{p}{2} \begin{pmatrix} a_0^{in} \\ \vdots \\ a_6^{in} \end{pmatrix} ; \quad (34)$$

matrix elements are functions of  $(a_0, a_1, \dots, a_6)$

where the explicit form of the matrix elements in terms of the classical steady state amplitudes  $(a_0, a_1, \dots, a_6)$  is given in Appendix A. The input fluctuation operators at RHS are in the vacuum state and have commutation relations as those in Eq.(15). This represents a 14 × 14 linear problem, which is trivial from a numeric point of view; however, when searching for some explicit combination of mode operators that has sub-shot-noise fluctuations, the problem seems too complex to find analytical solutions. Nevertheless, some hints came from the analysis of the classical steady state.

We integrated numerically the set of classical equations (33), and looked at the long time behaviour of the mode amplitudes. Above the critical point (11) the hexagonal steady-state of the classical equations of the model

$$E_s(\mathbf{x}) = \frac{1}{b} a_0 + \frac{1}{b} \sum_{i=1}^6 a_i e^{i\mathbf{k}_i \cdot \mathbf{x}} ; \quad (35)$$

is characterized by:

{ All the hexagonal modes have the same mean intensity

$$|a_1|^2 = |a_2|^2 = \dots = |a_6|^2 = |a_j|^2 ; \quad (36)$$

so that we set  $a_j = |a_j| e^{i\phi_j}$ . Figure 3a shows the steady-state hexagonal mode amplitude  $|a_j|^2$  as a function of the input field intensity. The figure is obtained by integrating the classical mode equations (33) under a slow (with respect to the characteristic time needed to reach the steady state) increasing of the input field intensity across the instability threshold (solid curve); the dashed curve correspond to a slow decrease of the input intensity. As it is well known [4,15] the instability is subcritical, and the hexagonal mode amplitude shows the typical hysteresis cycle. Figure 3b is the same for the amplitude  $|a_0|^2$  of the homogeneous mode.

{ The sums of the phases of symmetric modes are all equal

$$\phi_1 + \phi_4 = \phi_3 + \phi_6 = \phi_5 + \phi_2 = 2\pi ; \quad (37)$$

{ The differences of the phases of symmetric modes sum up to zero<sup>2</sup>

<sup>2</sup>Notice that in the classical analysis presented in [4,15], some initial assumptions on the steady state were made so that condition (37) was automatically fulfilled, with  $\phi = 0$ , and condition (38) was written as  $(\phi_1 + \phi_3 + \phi_5) = 2\pi = 0$ .

$$\phi_1 + \phi_3 + \phi_5 = 0 \text{ with } \phi_j = \phi_j - \phi_3 : \quad (38)$$

There are two phases which are not fixed by the steady-state equations, namely two of the phase differences between symmetric modes, say  $\phi_1$  and  $\phi_3$ . The value of these phases at steady-state depends only on initial conditions, and these variables are dominated by noise. This circumstance is a noteworthy consequence of the translational symmetry of the model, broken by the formation of the pattern in the transverse plane. As a matter of fact, for each value of the input field intensity  $J_I^2$  above the critical point, there exists a continuous set of steady-state solutions of the mode equations (33), of the form

$$E_s(\mathbf{x}) = \frac{1}{b} e^{i\phi_0} + \frac{2}{b} \sum_j e^{i\phi_j} \cos \mathbf{k}_1 \cdot \mathbf{x} + \phi_1 + \cos \mathbf{k}_3 \cdot \mathbf{x} + \phi_3 + \cos \mathbf{k}_5 \cdot \mathbf{x} + (\phi_1 + \phi_3) e^{i\phi_0} \quad (39)$$

corresponding to an arbitrary choice of  $\phi_1, \phi_3$ . By setting  $\phi_1 = \mathbf{k}_1 \cdot \mathbf{x}$ , and  $\phi_3 = \mathbf{k}_3 \cdot \mathbf{x}$ , we notice that  $\phi_1 + \phi_3 = (\mathbf{k}_1 + \mathbf{k}_3) \cdot \mathbf{x} = \mathbf{k}_5 \cdot \mathbf{x}$ . Thus the set of solutions (39) corresponds to the continuous set of rigid translations of the hexagonal pattern in the  $(x, y)$  plane,  $\mathbf{x} \rightarrow \mathbf{x} + \mathbf{x}$ .

As it is common in continuous symmetry breaking phase transition [30] close to the critical point, the noise is concentrated on the mode that aims to restore the symmetry broken by the transition. In our case we argue that close to the instability threshold, quantum fluctuations corresponding to rigid translations of the pattern result in huge fluctuations of the differences of the phases between symmetric modes  $\phi_j$ , but leaves invariant the quantities

$$(A) \quad \phi_1 + \phi_3 + \phi_5 \quad (40)$$

$$(B) \quad (\phi_i + \phi_{i+3}) - (\phi_{i+1} + \phi_{i+4}) \quad i = 1; \dots; 6 \quad (41)$$

Hence, our possible candidates for squeezing are the observables

$$(a_1 - a_4 + a_3 - a_6 + a_5 - a_2) e^{i\phi_0} + h.c.; \quad (42)$$

which corresponds to the classical quantity (A) in (40) for  $\phi_0 = \phi_0 + \pi/2$ , and

$$[(a_1 + a_3) - (a_{1+1} + a_{1+4})] e^{i\phi_0} + h.c.; \quad (43)$$

which corresponds to (B) in (41) when  $\phi_0 = \phi_0 + \pi/2$ . In these definitions  $\phi_j$  are left arbitrary and will be used as optimization parameters.

In addition, an obvious observable to take into account is

$$[(a_1 - a_3) + (a_{1+1} - a_{1+4})] e^{i\phi_0} + h.c. \quad i = 1; 2; \quad (44)$$

In the small quantum noise approximation, this observable corresponds to the photon number difference  $N_1 - N_2$ , which was shown in the previous section to have a sub-shot noise fluctuation spectrum.

Luckily enough, when considering the combinations of mode quadratures given by (42), (43), (44), their dynamical equations decouple from the other equations of the system (34), and we are left with 2  $\times$  2 linear problems.

Before examining specific cases, we note that the quantum dynamics of a generic linear system can be written as

$$\frac{d}{dt} V = M V + \frac{P}{2} \overline{V}^{in}; \quad (45)$$

where  $V, V^{in}$  are the system and noise operators vectors respectively, while  $M$  is a coefficient matrix.

Suppose that the components of the vector  $V$  are two conjugate field quadratures  $Z(0)$  and  $Z(\pi/2)$ ; at steady state the system can be solved in the frequency domain, and, with the aid of an input-output relation [13]

$$V^{out} = \frac{P}{2} \overline{V} - V^{in}; \quad (46)$$

it is possible to calculate the output correlation matrix. In the frequency domain it reads

$$C^{out}(\omega) = \int_0^T d\omega' \langle V^{out}(\omega') [V^{out}(\omega - \omega')]^\dagger \rangle = \frac{h}{2} (M + i\omega I)^{-1} + \frac{h}{2} C^{in}(\omega) \frac{h}{2} (M - i\omega I)^{-1} + \frac{h}{2} I; \quad (47)$$

where  $I$  is the identity matrix,  $T$  means the transpose, and  $C^{in}(\omega) = \int_0^R d\omega' \langle V^{in}(\omega') [V^{in}(\omega - \omega')]^\dagger \rangle$  is the input correlation matrix.

Moreover, the noise spectrum of a generic quadrature



$$Z(\varphi) = Z(0) \cos \varphi + Z(\varphi=2) \sin \varphi; \quad (48)$$

is given by

$$S_Z(\varphi; I) = \frac{1}{2} \langle Z^{\text{out}}(\varphi; I) Z^{\text{out}}(\varphi; I)^{\dagger} \rangle \quad (49)$$

$$= C_{1;1}^{\text{out}}(I) \cos^2 \varphi + C_{2;2}^{\text{out}}(I) \sin^2 \varphi + C_{1;2}^{\text{out}}(I) + C_{2;1}^{\text{out}}(I) \sin \varphi \cos \varphi; \quad (50)$$

With the above in mind we are now going to consider specific cases.

#### A. Noise in the sum of phase differences

Let us consider the quadrature operator

$$W(\varphi) = \frac{1}{\sqrt{6}} (a_1 - a_4 + a_3 - a_6 + a_5 - a_2) e^{i\varphi} + \text{h.c.}; \quad (51)$$

The dynamics of the fluctuation vector  $V = [W(0); W(\varphi=2)]^T$ , gives rise to a closed system like (45), with

$$M = \begin{pmatrix} \text{Re} f_A + g & \text{Im} f_A + g \\ \text{Im} f_A - g & \text{Re} f_A - g \end{pmatrix}; \quad (52)$$

and

$$A = \begin{pmatrix} 1 - 2i + 2ij_0 j^2 + 10ij_j^2 & 4i_0 & 4i_0 \\ 4i_0 & 5i(\varphi)^2 + i(\varphi_0)^2 & \end{pmatrix}; \quad (53)$$

In writing (53) the symmetries of the steady state have been taken into account; moreover, among the possible stationary states (39) we used the one corresponding to  $\varphi_1 = 0$ ,  $\varphi_3 = 0$ . The input correlation matrix is given by

$$C^{\text{in}} = \begin{pmatrix} 1 & i \\ i & 1 \end{pmatrix}; \quad (54)$$

We performed calculations of the noise spectrum  $S_W(\varphi; I)$  for various values of the input beam intensity  $I_{\text{in}}^j$  in the region where the hexagonal solution exists. The amplitudes of the homogeneous mode  $\varphi_0$ , and of the hexagonal mode were obtained both by numerically integrating the dynamical classical equations (33) and looking at the long time behavior, and by numerically solving the nonlinear steady-state equations (see Appendix B). An excellent agreement between the two approaches was found.

Figure 4 shows an example of the typical results. Part A1 of the figure plots the zero frequency spectrum as a function of the quadrature angle  $\varphi$ , shifted by  $\varphi=2$ . Sub-shot-noise fluctuations are present for a rather broad range of quadrature angles; it has to be noticed that the quadrature operator exactly corresponding to the classical sum of phase differences (40) is the one with  $\varphi + \varphi=2 = \varphi_0$  where  $\varphi_0$  is the steady-state phase of  $\varphi$  (indicated by arrows in the figure). Hence sub-shot noise fluctuations are present for quadratures somehow rotated with respect to the semiclassical "phase" quadrature. In Part A2 of the figure the quadrature angle is chosen to optimize squeezing; the plots evidenciate the typical Lorentzian shape of the fluctuation spectrum.

Line (A) in figure 7 plots the best squeezing (that is, the low frequency noise with the phase optimized) as a function of the input field intensity, and shows that sub-shot noise fluctuations for this observable are present in the whole region where the hexagonal solution exists.

#### B. Noise in the difference of phase sums

We consider now the quadrature operators

$$Q(\varphi) = \frac{1}{\sqrt{4}} (a_1 + a_{i-3} - a_{i-1} - a_{i-4}) e^{i\varphi} + \text{h.c.}; \quad (55)$$

In fact there are two independent mode combinations of this form, e.g. for  $i = 1; 2$ , and for both of them we get a closed system like (45) for the fluctuation vector  $V = [Q(0); Q(\varphi=2)]^T$ , with

$$M = \begin{pmatrix} \text{Re}fB_+ g & \text{Im}fB_+ g \\ \text{Im}fB_- g & \text{Re}fB_- g \end{pmatrix}; \quad (56)$$

and

$$B = \begin{pmatrix} 1 & 2i + 2ij_0 f^2 + 6ij f^2 & 2i_0 & 2i_0 \\ 2i_0 & 3i(\ )^2 & i(\ )^2 & \end{pmatrix}; \quad (57)$$

The input noise correlations are again given by (54). Fig.5 shows the noise spectrum  $S_Q(\omega; \theta)$ , and is analogous to Fig.4. As in the previous case, the spectrum has a Lorentzian shape and exhibits squeezing in the whole region where hexagons are predicted by the seven mode model, although the squeezed quadratures do not exactly coincide with the one corresponding to the classical phases in (41).

Line (B) in figure 7 plots the best squeezing as a function of the input field intensity, and shows that also in this case sub-shot noise fluctuations for this observable are present in the whole region where the hexagonal solution exists.

#### C. Noise in the sum of intensity differences

Finally, let us consider the two independent quadratures

$$X(\omega) = \frac{1}{\sqrt{4}} [(a_1 + a_{i-3}) - (a_{i-1} + a_{i-4})] e^{-i\omega t} + \text{h.c.}; \quad i=1,2; \quad (58)$$

Again, their fluctuation vectors  $V = [X(0); X(\omega=2)]^T$ , give rise to two closed systems like (45) with

$$M = \begin{pmatrix} \text{Re}fC_+ g & \text{Im}fC_+ g \\ \text{Im}fC_- g & \text{Re}fC_- g \end{pmatrix}; \quad (59)$$

and

$$C = \begin{pmatrix} 1 & 2i + 2ij_0 f^2 + 10ij f^2 + 2i_0 & 2i_0 \\ 2i_0 & 5i(\ )^2 + i(\ )^2 & \end{pmatrix}; \quad (60)$$

The input correlation matrix is the same of Eq.(54).

It is worth noting that the quadrature corresponding to the hexagonal mode stationary phase satisfies a simple equation

$$\frac{d}{dt} X(\omega) = -2 X(\omega) + \frac{p}{2} X^{\text{in}}; \quad (61)$$

which gives a Lorentzian shape spectrum

$$S_X(\omega; \theta) = \frac{p^2}{4\omega^2 + p^2}; \quad (62)$$

Taking into account that now the shot-noise level is scaled to 1, this is in perfect agreement with the results of Section II, since  $X(\omega)$  represents the linearized version of the observable  $N$ .

It is interesting to remark that, differently with respect to the previous cases, for this combination of modes the low frequency noise reduction abruptly disappears when the quadrature is slightly rotated with respect to the amplitude quadrature. In fact, as shown by figure 6, a large positive peak located at zero frequency appears on the Lorentzian spectrum when the quadrature angle is shifted from  $\theta = 0$ .

Line (C) in figure 7 plots a numerical evaluation of the best squeezing as a function of the input field intensity. As it is obvious from the analytical formula (62) complete noise suppression is predicted at zero frequency for  $\theta' = 0$  (the amplitude quadrature), in the whole region where the hexagonal solution exists.

In conclusion, we have studied the quantum features underlying the hexagonal pattern formation in a Kerr cavity. We have identified a rich scenario of purely quantum correlations among the  $o$ -axis modes that form the hexagonal pattern. In fact we have shown that at least five independent combinations of mode observables exhibit sub-shot-noise fluctuations.

We believe that the six-mode entanglement analysed in this paper might be of great interest. On the one side this kind of patterns are widely studied in labs, so that it should be easy to look for the described quantum effects. On the other side, the quantum properties of such systems make them good candidates for quantum information processing with continuous variable [27,29,31]. In particular, the existence of several observables showing correlations at the quantum level opens the possibility of distilling a considerable amount of entanglement in practical situations, and to use it.

In this connection an interesting question is whether this kind of spatial entanglement is characteristic of the particular model analysed here, or it is in general typical of the hexagonal pattern, independently of the detailed mechanism that underlie its formation. Further investigations about models closer to experimental situations where hexagons have been found are hence in order.

Another interesting point concerns the possibility that some squeezing is missing from our picture. The symmetry of the problem suggests the possibility that quantum correlations – more probably anti-correlations – exist between the sum of all hexagonal modes and the pump mode. This would be closely similar to the situation analysed in [32,33], in the context of a self-defocusing Kerr cavity, where quantum anticorrelations were found between the pump on-axis intensity and the intensities of two symmetrical  $o$ -axis modes.

Another open question is whether these quantum correlations survive when including in the model the full continuum of transverse modes. As a matter of fact, being the bifurcation subcritical, the hexagonal mode emerges at threshold with a finite amplitude. Hence higher order spatial harmonics might have a non-negligible amplitude even in the neighbourhood of the threshold, and photon scattering in these additional modes might spoil our correlations. This will be the subject of future numerical investigations.

#### ACKNOWLEDGMENTS

The authors warmly thank L.A. Lugiato for useful suggestions and constant encouragement. This work was carried out in the framework of the network QSTRUCT of the EU TM R programme. S.M. acknowledges financial support from the MURST project "Spatial pattern control in nonlinear optical systems"

#### APPENDIX A

In this Appendix we give the explicit form of the linear system (34) for the dynamics of fluctuations of the hexagonal modes. In writing these equations we took into account the symmetries of the hexagonal steady state expressed by conditions (36), (37) and (38); moreover among the possible steady states in (39) we choose for simplicity the one with  $\phi_j = 0$ ,  $j = 1; 3; 5$  (this corresponds to fixing the origin of the coordinate axes in the transverse plane). We get

$$\begin{aligned} \frac{1}{dt} \dot{a}_0 = & -1 - i + 2ij_0 \dot{f} + 12ij \dot{f}^2 a_0 + i_0^2 + 6i^2 a_0^y \\ & + 2i_0 + 2i_0 + 4ij \dot{f}^2 \sum_{j=1}^6 X^6 a_j + [2i_0] \sum_{j=1}^6 X^6 a_j^y + \frac{r}{2} a_0^{in}; \end{aligned} \quad (63)$$

$$\begin{aligned} \frac{1}{dt} \dot{a}_j = & 2i_0 + 2i_0 + 4ij \dot{f}^2 a_0 + 2i_0 + 2i^2 a_0^y \\ & + 1 - 2i + 2ij_0 \dot{f} + 12ij \dot{f}^2 a_j + i^2 a_j^y \\ & + 2i_0 + 2i_0 + 4ij \dot{f}^2 a_{j-1} + 2i^2 a_{j-1}^y \\ & + 4ij \dot{f}^2 a_{j-2} + 2i_0 + 2i^2 a_{j-2}^y \\ & + 2ij \dot{f}^2 a_{j-3} + i_0^2 + 6i^2 a_{j-3}^y \\ & + 4ij \dot{f}^2 a_{j-4} + 2i_0 + 2i^2 a_{j-4}^y \\ & + 2i_0 + 2i_0 + 4ij \dot{f}^2 a_{j+5} + 2i^2 a_{j+5}^y + \frac{r}{2} a_j^{in}; \quad j = 1; \dots; 6: \end{aligned} \quad (64)$$

The elements of the matrices  $M$  can be built up by appropriately combining some of the above equations.

## APPENDIX B

This appendix gives the explicit expression of the nonlinear equations for the classical hexagonal steady-state. These are obtained by equating to zero the l.h.s of Eqs.(33); in order to find a numerical solution we transformed them in four nonlinear equations for the real variables  $u_0; v_0; u_1; v_1$  introduced as [15]

$$0 = E_{0s} + E_{0s} (u_0 + iv_0) ; \quad (65)$$

$$= \frac{E_{0s}}{2} (u_1 + iv_1) ; \quad (66)$$

The resulting equations are

$$\begin{aligned} 0 = & u_0 + (E_{0s})^2 v_0 - E_{0s}^2 2u_0 v_0 + u_1 v_1 + u_0^2 v_0 + \frac{1}{2} v_0 u_1^2 \\ & + \frac{1}{2} u_1^2 v_1 + u_0 u_1 v_1 + v_0^3 + \frac{3}{2} v_0 v_1^2 + \frac{1}{2} v_1^3 ; \end{aligned} \quad (67)$$

$$\begin{aligned} 0 = & v_0 - (E_{0s})^2 u_0 + E_{0s}^2 2u_0 + 3u_0^2 + \frac{3}{2} u_1^2 + v_0^2 + \frac{1}{2} v_1^2 + u_0^3 \\ & + \frac{3}{2} u_0 u_1^2 + \frac{1}{2} u_1^3 + u_0 v_0^2 + \frac{1}{2} u_0 v_1^2 + v_0 u_1 v_1 + \frac{1}{2} u_1 v_1^2 ; \end{aligned} \quad (68)$$

$$\begin{aligned} 0 = & u_1 + 2v_1 - E_{0s}^2 v_1 2u_0 v_1 + 2v_0 u_1 + \frac{2}{3} u_1 v_1 + \frac{1}{3} v_0 u_1^2 \\ & + 2u_0 v_0 u_1 + u_0^2 v_1 + \frac{5}{4} u_1^2 v_1 + \frac{2}{3} u_0 u_1 v_1 + 3v_0^2 v_1 + \frac{2}{3} v_0 v_1^2 + \frac{5}{4} v_1^3 ; \end{aligned} \quad (69)$$

$$\begin{aligned} 0 = & v_1 - 2u_1 + E_{0s}^2 3u_1 + 6u_0 u_1 + \frac{2}{3} u_1^2 + 2v_0 v_1 + \frac{1}{3} v_1^2 \\ & + 3u_0^2 u_1 + \frac{2}{3} u_0 u_1^2 + \frac{5}{4} u_1^3 + 2u_0 v_0 v_1 + \frac{1}{3} u_0 v_1^2 + v_0^2 u_1 + \frac{2}{3} v_0 u_1 v_1 + \frac{5}{4} u_1 v_1^2 ; \end{aligned} \quad (70)$$

The above equations are solved numerically with the help of Mathematica, by using, for simplicity, the condition  $E_{0s} = E_{in}$ , which assures that  $E_{in} = E_{0s}$  (see Eq. (10)). The solutions are compared to the steady-state mode amplitudes obtained by numerically integrating the dynamical equations (33); a perfect agreement between the two approaches has been found.

- [1] For a review, see for example (a) L.A. Lugiato, Chaos Solitons Fractals 4, 1251 (1994), and references quoted therein; (b) L.A. Lugiato, M. Brambilla and A. Gatti, in Advances in Atomic Molecular and Optical Physics 40, 229, B. Bederson and H. Walther eds. (Academic Press, New York, 1998).
- [2] W.J. Firth and C. Pare, Opt. Lett. 13, 1096 (1988)
- [3] W.J. Firth, J. Mod. Opt. 37, 151 (1990); G.P. D'Alessandro and W.J. Firth, Phys. Rev. A 46, 537 (1992).
- [4] W.J. Firth, A.J. Scroggie, G.S. McDonald and L.A. Lugiato, Phys. Rev. A 46, R3609 (1992).
- [5] W.J. Firth and A.J. Scroggie, Europhys. Lett. 26, 521 (1994)
- [6] G. Grynberg, E. Le Bihan, P. Verkerk, P. Simonneau, J.R.R. Leite, D. Bloch, S. Le Boiteux and M. Ducloy, Opt. Comm. 67, 363 (1988)

- [7] T. Ackemann, Yu. a. Logvin, A. Heuer and W. Lange, Phys. Rev. Lett. 75, 3450 (1995); E. Pampaloni, S. Residori and F. T. Arecchi, Europhys. Lett. 24, 647 (1993); R. Neubecker, B. Thuerling and T. Tschudi, chaos Solitons and Fractals 4, 1307 (1994)
- [8] L. A. Lugiato and R. Lefever, Phys. Rev. Lett. 58, 2209 (1987).
- [9] L. A. Lugiato and R. Lefever, Phys. Rev. Lett. 58, 2209 (1987).
- [10] G. Grynberg and L. A. Lugiato, Opt. Comm. 101, 69 (1993).
- [11] L. A. Lugiato and F. Castelli, Phys. Rev. Lett. 68, 3284 (1992).
- [12] R. Bonifacio and L. A. Lugiato, Lett. Nuovo Cimento 21, 505 (1978).
- [13] C. W. Gardiner, Quantum Noise, (Springer, Berlin, 1991).
- [14] H. M. Gibbs, S. L. McCall and T. N. C. Venkatesan, Phys. Rev. Lett. 36, 113 (1976).
- [15] A. J. Scroggie, W. J. Firth, G. S. McDonald, M. Tlidi, R. Lefever and L. A. Lugiato, Chaos, Solitons and Fractals 4, 1323 (1994).
- [16] G. Grynberg, Opt. Comm. 66, 321 (1988)
- [17] J. B. Geddies, J. V. Moloney, E. M. Wright and W. J. Firth, Opt. Comm. 111, 623 (1994).
- [18] M. Hoyuelos, P. Colet, M. San Miguel and D. W. Algraef, Phys. Rev. E 58, 2992 (1998).
- [19] G. -L. Oppo, M. Brambilla, and L. A. Lugiato, Phys. Rev. A 49, 2028 (1994); G. -L. Oppo, M. Brambilla, D. Casasas, A. Gatti and L. A. Lugiato, J. Mod. Opt. 41, 1151 (1994).
- [20] S. Reynaud, C. Fabre and E. Giacobino, J. Opt. Soc. Am. B 4, 1520 (1987).
- [21] A. Gatti, H. Wiedemann, L. A. Lugiato, I. Marzoli, G. -L. Oppo and S. M. Barnett, Phys. Rev. A 56, 877 (1997).
- [22] I. Marzoli, A. Gatti and L. A. Lugiato, Phys. Rev. Lett. 78, 2092 (1997).
- [23] C. Szwaj, G. -L. Oppo, A. Gatti and L. A. Lugiato, Eur. Phys. J. D., 10, 433 (2000).
- [24] A. Gatti, E. Brambilla, L. A. Lugiato and M. I. Kolobov, J. Opt. B: Quant. Sem. Opt., 196-203 (2000).
- [25] M. D. Reid and P. D. Drummond, Phys. Rev. Lett. 60, 2731 (1988); Z. Y. Ou, S. F. Pereira and H. J. Kimble, Appl. Phys. B, 55, 265 (1992).
- [26] A. Gatti, L. A. Lugiato, K. J. Petsas and I. Marzoli, Europhys. Lett. 46, 461.
- [27] S. L. Braunstein and H. J. Kimble, Phys. Rev. Lett. 80, 869 (1998)
- [28] M. Reid, Phys. Rev. A 62, 062308 (2000); P. Navez, A. Gatti and L. A. Lugiato, quant-ph/0101113.
- [29] S. Lloyd and S. Braunstein, Phys. Rev. Lett. 82, 1784 (1999).
- [30] D. Forster, Hydrodynamic Fluctuations, Broken Symmetry, and Correlation Functions, (Benjamin, New York, 1975).
- [31] Quantum Information Theory with Continuous Variables, S. Braunstein and A. Pati eds. (Kluwer, New York, 2001).
- [32] M. Hoyuelos, A. Sinatra, P. Colet, L. Lugiato and M. San Miguel, Phys. Rev. A 59, 1622 (1999).
- [33] R. Zambrini, M. Hoyuelos, A. Gatti, P. Colet, L. Lugiato and M. San Miguel, Phys. Rev. A 62, 063801 (2000).

# V I. F I G U R E S

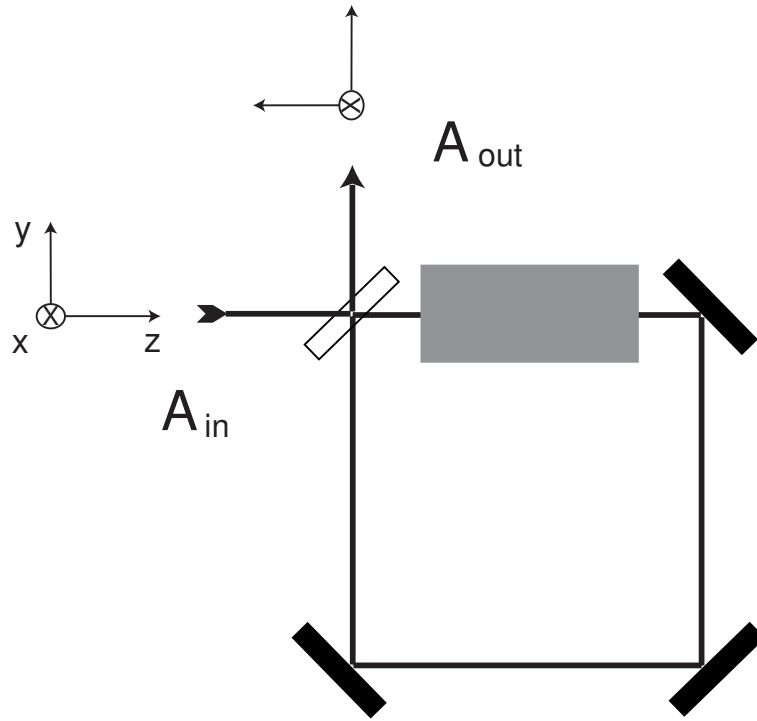


FIG .1. Scheme of a ring cavity containing a Kerr medium (K ). The longitudinal and transverse axis are shown for both input and output eld.

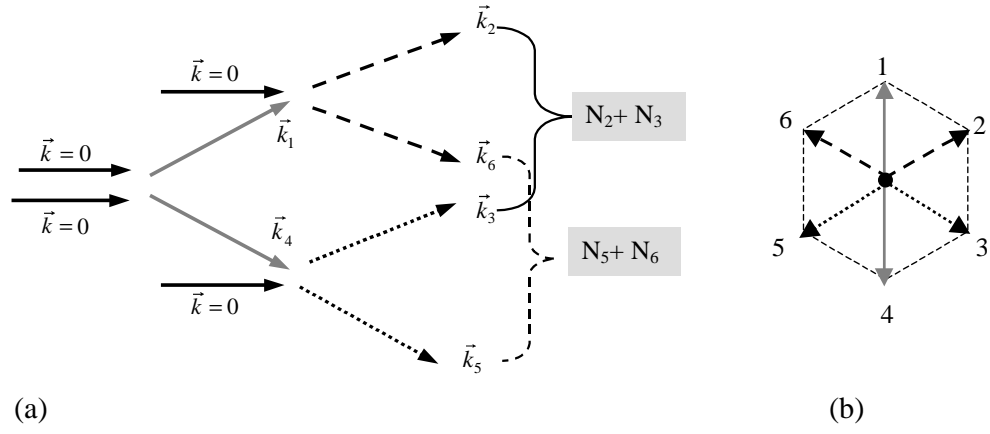


Fig. 2

FIG. 2. (a) Scheme of the microscopic processes leading to hexagonal pattern generation (see text). (b) Transverse wave vectors forming the hexagonal pattern.

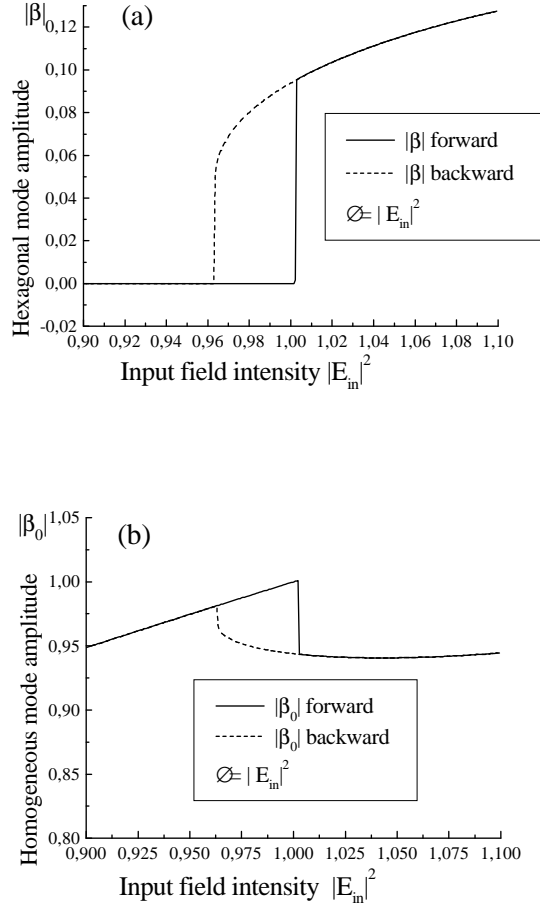


Fig.3

FIG. 3. Example of the steady-state curves for the hexagonal mode (a) and the homogeneous mode (b) amplitudes as a function of the input beam intensity. Solid (dashed) lines are obtained by a numerical integration of Eqs.(33) over times long compared to time scales of dynamical evolution, and by a slow forward (backward) sweep of the input beam intensity across the instability threshold ( $|E_{in}|^2 = 1$ ). Cavity detuning is chosen as  $\delta = \delta_{0s} \sqrt{2}$ .



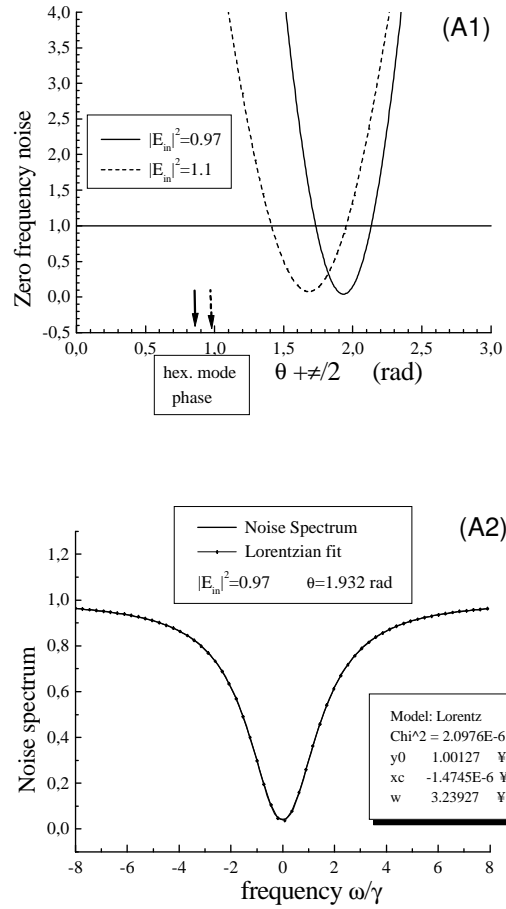


Fig.4

FIG. 4. Part (A1) shows the zero frequency spectrum of the observable  $W(\theta)$ , given by Eq.(51), vs the quadrature angle shifted by  $\pi/2$ , for two values of the input field. The arrows indicate the corresponding hexagonal mode phases. Part (A2) shows the frequency spectrum for the optimal value of quadrature angle.  $\theta = \theta_{opt}$ . Other parameters are indicated in the figure. Dots correspond to a Lorentzian fit.

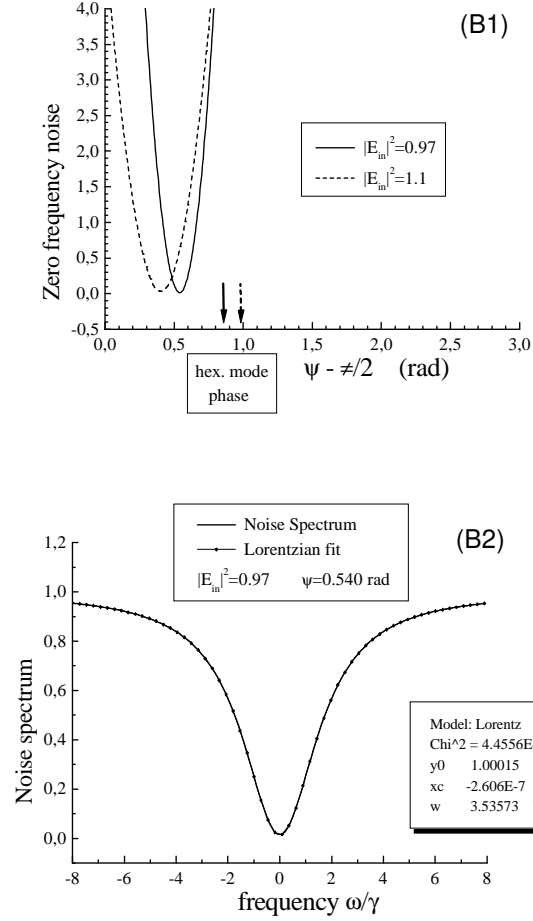


Fig.5

FIG. 5. Part (B1) shows the zero frequency spectrum of the observable  $Q$  ( ) given by Eq.(55), vs the quadrature angle shifted by  $\pi/2$ , for two values of the input field. The arrows indicate the corresponding hexagonal mode phases. Part (B2) shows the frequency spectrum for the optimal value of quadrature angle,  $\psi = \pi/4$ . Other parameters are indicated in the figure. Dots correspond to a Lorentzian fit.

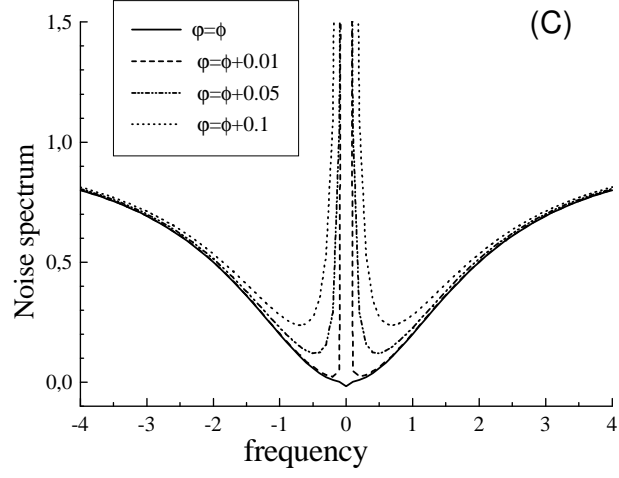


FIG. 6. Noise spectrum of the observable  $X(\phi')$  given by Eq.(58). The solid line is the Lorentzian spectrum when the quadrature angle  $\phi' = \phi$ ; the other lines correspond to quadratures slightly rotated with respect to the amplitude quadrature, as indicated in the figure.

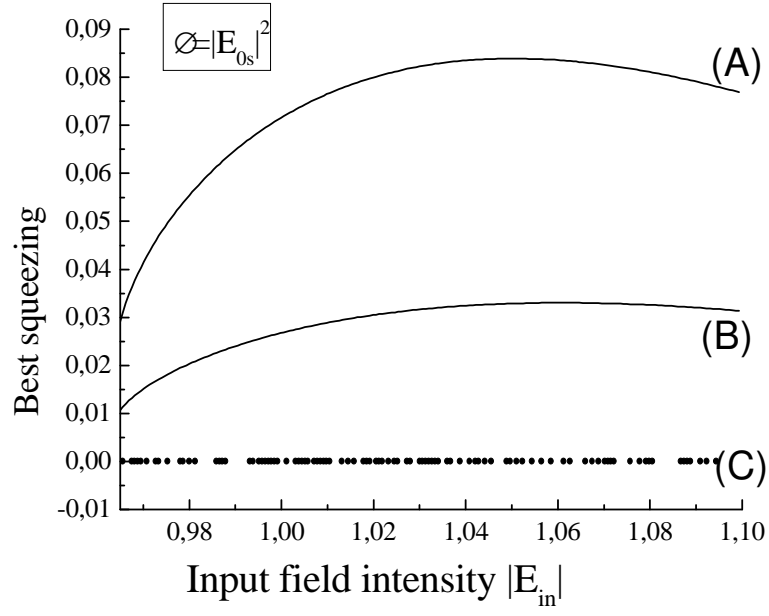


FIG . 7. Best squeezing (low frequency noise with the quadrature angle optimized) as a function of the input field intensity, for the three observables considered in Sections IV A (line A ), IV B (line B ), and IV C (line C ).